Denaturation of Lysozyme and Myoglobin in Laser Spray

Atsushi Takamizawa, Susumu Fujimaki, Jan Sunner,* and Kenzo Hiraoka

Clean Energy Research Center, University of Yamanashi, Kofu, Japan

In laser spray, the tip of an electrospray capillary is irradiated with a continuous CO_2 laser beam. Here, we report results from a modified laser spray method that employs a relatively low laser irradiance level. With a laser power of ~2 W and a focal spot size (~0.3 mm), which covered the entire front surface of the electrospray capillary, the irradiance was $\sim 3 \times 10^3$ W/cm^2. This resulted in a quiescent and smooth vaporization of aqueous solutions. This "evaporation-mode" laser spray method yielded the best results so far obtained in our laboratory with laser-irradiated electrospray, producing higher and more stable signals. The method was applied to the analysis of aqueous solutions of lysozyme and myoglobin. Mass spectra were obtained as a function of laser power from 0 W (electrospray) to ~2 W. The spray generated at the tip of the stainless steel capillary was observed with a CCD camera. With increase of laser power, the droplets in the spray became finer and the Taylor cone became progressively smaller. The strongest ion signals were recorded when the sample solution protruded only slightly from the tip of the capillary. A broadening of the lysozyme charge-state distribution, attributable to protein unfolding, was observed with a laser power of 2 W. No denaturation of myoglobin took place up to a laser power of 1.6 W. However, a sudden onset of denaturation was observed at 1.8 W as a broadening of the myoglobin charge distribution and the appearance of apo-myoglobin peaks. These findings demonstrate that laser spray is capable of dissociating the noncovalent complexes selectively without breaking covalent bonds. (J Am Soc Mass Spectrom 2005, 16, 860–868) © 2005 American Society for Mass Spectrometry

Fundamentally different strategies, i.e., energy-sudden activation, nebulization, and the application of high electric fields, are employed in modern mass spectrometry (MS) for the formation of gaseous ions from condensed phase. While electrospray makes use of nebulization and high electric fields, but not energy-sudden activation, MALDI is primarily based on energy-sudden activation. The combination of all three strategies in one experiment holds great promise.

Energy-sudden activation MS methods are closely related to the concept of "limit of superheat". When a liquid is heated slowly, vapor bubble formation typically occurs from vapor nucleation sites, i.e., heterogeneous nucleation. Such sites are ubiquitous on rough solid surfaces. Suppression of heterogeneous nucleation can be achieved by suspending droplets of the volatile liquid in another liquid with which it doesn't mix. Alternatively, a liquid can be heated or depressurized rapidly enough, so that there is insufficient time for vapor bubbles to form at nucleation sites. Under such conditions, a liquid can be heated to temperatures far above its boiling point. However, at the "limit of superheat", the rate of homogeneous nucleation rapidly increases. The limit of superheat is, as a rule, only about 10% below the critical temperature (T_c) ($T_{\text{superheat}} \approx 0.9T_c$) [1]. When extreme superheating takes place, evaporative fluxes, fluid accelerations, and departures from thermodynamic equilibrium are orders of magnitude greater than in ordinary boiling. The resulting explosive process is known as a vapor explosion [2]. Kafalas and Ferdinand studied vaporization and fragmentation of water (fog) droplets at atmospheric pressure by irradiation with a 10.6 μm, CO_2 laser pulse [3]. In the larger droplets (> ~40 μm diameter), front surface vaporization, accompanied by spallation of the droplet at its back surface, was observed. In contrast, smaller droplets (< ~20 μm diameter) underwent volume heating rather than front-surface heating and were found to vaporize completely. In related work, Hiraoka et al. irradiated liquid beams at atmospheric pressure with a continuous 10.6 μm laser beam perpendicular to the liquid beam [4]. The produced ions were sampled into vacuum and analyzed in a quadrupole mass spectrometer. The authors found that when the liquid water beam had a diameter larger than 50 μm, plumes (jet-like streams) were ejected in opposite directions from both

Published online March 30, 2005

Address reprint requests to Dr. K. Hiraoka, Clean Energy Research Center, University of Yamanashi, Takeda 4-3-11, Kofu 400 8511, Japan. E-mail: hiraoka@ab11.yamanashi.ac.jp

* On sabbatical leave from Montana State University, Bozeman, MT, USA.

1044-0305/05/$30.00
doi:10.1016/j.jasms.2005.02.012

Received August 24, 2004
Revised January 28, 2005
Accepted February 16, 2005

the illuminated and the shadow faces of the beam. When the liquid beam had a diameter of ≤20 μm, the laser-generated plume became nondirectional, and the droplets formed became much finer. These results are in good agreement with the study of Kafalas and Ferdinand [3].

Hiraoka et al. [4] reported that the minimum irradiation time required for explosive vaporization of the liquid water beam was ~0.7 μs at a laser power density of 6×10^5 W/cm^2. This corresponds to an energy deposition density of 420 J/cm^3, which is close to the energy required to reach the limit of superheat. However, it is considerably below the energy density required to fully vaporize the water stream. These results show that the limit of superheat is easily reached using also continuous laser irradiation, at least at atmospheric pressure conditions.

Wattenburg et al. have also studied laser irradiation of liquid beams as a source of ions [5, 6]. In their method, a water beam is injected into a vacuum chamber through a 10 μm nozzle and irradiated with a pulsed laser. The ions are analyzed using a time-of-flight mass spectrometer. It was found that intact noncovalent protein complexes, including intact hemoglobin [5] could be desorbed into the gas phase. Even water bound into cavities of intact proteins was detected, which demonstrates the extreme softness of this ionization approach.

The results of Hiraoka et al. [4] and Wattenberg et al. [5, 6] clearly showed that direct laser irradiation of aqueous solutions is an extremely promising approach for biochemical mass spectrometry. However, a major problem with using liquid beams is the very low efficiency of ionization. Therefore, it is essential to investigate alternative approaches. In the aqueous beam work conducted in this laboratory [4], it was observed that the ion signal increased with increasing voltage applied to the liquid beam. For this reason, laser irradiation of electrically charged surfaces has been actively pursued in our laboratory by irradiating aqueous solutions flowing out of an electrospray capillary with a continuous CO_2 laser at 10.6 μm. The resulting method is referred to as "laser spray".

In our early laser spray research [7], the working hypothesis was that the liquid should undergo homogeneous heating in order to reach the "limit of superheat" and achieve maximum ionization efficiency. Hence, only the liquid sample and/or the sprayed, charged liquid droplets were irradiated but not the quartz or stainless steel capillary. Initially, only the tip of the Taylor cone was irradiated by a focused, 0.3 mm diameter laser beam at right angle to the stainless steel capillary. However, the ion signals were found to decrease as the Taylor cone became unstable at a laser power density of 7×10^4 W/cm^2. In subsequent experiments, the laser was defocused to a 3 mm diameter spot and moved to irradiate only the spray region, but not the Taylor cone [7]. It was then found that ion signals, for example of protonated arginine from a 10^{-5} M solution in $CH_3OH/H_2O/CCl_4$ (8:2:0.5, vol/vol), increased by as much as an order of magnitude at a laser power density of 7×10^2 W/cm^2 [7]. It is evident that the laser irradiation enhanced the vaporization of charged liquid droplets, presumably the larger droplets mainly found in the central region of the spray cone [8, 9], and that this lead to a more effective desorption of solvated ions into the gas phase. Unfortunately, the intensity increase was only achieved when the electrospray was stable. When using aqueous solutions, the Taylor cone was unstable and no increase in ion abundances was observed.

In 1995, the laser/electrospray experimental setup was modified by irradiating the electrospray coaxially, from the opposite side of the capillary, with the 10.6 μm infrared CO_2 laser. To minimize direct heating of the metal, the laser beam was focused to a 0.1 mm spot, which was slightly smaller than the inner diameter (0.13 mm) of the capillary [10–15]. With aqueous solutions, the limit of superheat was reached with a laser power of 10 W (power density 1.3×10^5 W/cm^2), as evidenced by explosive vaporization and mist formation visible to the naked eye [10–15]. Because of the high laser power density used, the centering of the laser focal spot onto the tip of the stainless steel capillary was critical for obtaining reproducible ion signals. A slight off-center adjustment caused the tip of the stainless steel capillary to melt. Depending on the composition of the sprayed solution, the change in ion abundances ranged from dramatic, with an increase by several orders of magnitude, to insignificant. Laser spray represents a hybrid of the three fundamental approaches for the formation of gaseous ions from the condensed phase, i.e., energy-sudden activation, nebulization, and the application of a high electric field [11]. Since the solvent also acts as a laser-desorption matrix, laser spray may be regarded as electric-field assisted MALDI.

The absorption coefficient of liquid water at a wavelength of 10.6 μm is about 10^3 cm^{-1} [16]. This rather high absorption coefficient enables rapid heating of the aqueous solution effusing out of the capillary by laser irradiation. In our previous report [11], a detailed investigation was made to determine whether thermally labile compounds (e.g., ribostamycin, acetylcholine chloride, and cholesterol 3-sulfate sodium salt) suffer from decomposition by the laser irradiation at a laser power density of $4–6 \times 10^4$ W/cm^2. No fragment ions were detected for the selected compounds. This showed that the temperature rise of the liquid was not high enough to cause bond dissociation of the thermally labile covalent bonds.

Recently, we have found that the performance of laser spray could be further improved, yielding stronger and more stable ion signals, by expanding the spot size of the focused laser beam to cover the outer diameter of the stainless steel capillary [17]. At the same time, the laser power density was decreased by more than an order of magnitude.

In the present work, the modified laser spray geom-

etry was employed to obtain laser spray mass spectra of aqueous solutions of lysozyme and myoglobin. Ions were analyzed using an orthogonal time-of-flight (TOF) mass spectrometer. It was found that laser spray induces the denaturation of lysozyme and myoglobin, i.e., the selective dissociation of noncovalent bonds in these proteins.

Experimental

The general experimental procedures are similar to those described previously [10, 17]. In brief, a stainless steel capillary (i.d.: 0.1 mm, o.d.: 0.2 mm) at atmospheric pressure is supplied with a sample solution by using a syringe pump (Harvard Apparatus, Type 11 Plus, Holliston, MA). The flow rate of the sample solution is 3–10 μL/min. The capillary is positioned parallel to the interface plate of the mass spectrometer. Nebulizer gas, N_2, effusing from a concentric stainless steel tube (i.d.: 0.7 mm) reduces the angular divergence of the plume and entrains the mist and gas in a confined gas stream going towards the sampling orifice. The flow rate of the N_2 nebulizer gas was optimized for the strongest ion signals. With laser off, the N_2 flow rate of 0.5 L/min was the best choice.

A Synrad Firestar V20, model FSV20SFB, laser (Synrad, WA) 20 W infrared laser (10.6 μm) is used. The tip of the stainless steel capillary is irradiated axially, from the opposite side of the capillary, by a laser beam focused to a ≈0.3 mm diameter spot with the laser power of up to 2.0 W. The beam is focused by a 200 mm focal length ZnSe lens. The power of the Synrad laser is varied by pulse-width modulation at a repetition frequency of 5 kHz. Essentially, the laser is turned on and off every 200 μs. Thus, the optical waveform consists of a series of pulses. However, the rise and fall time constant is about 100 μs, and for this reason the maximum instantaneous laser power is only about double the average power. At 2 W, the average laser power density is calculated to be 3×10^3 W/cm^2, with a maximum of about 1.2×10^4 W/cm^2. Laser power levels higher than 2 W were used only for limited time periods, or the tip of the stainless steel capillary would melt and change shape. The gaseous ions formed are sampled through a 400 μm diameter orifice into the vacuum system and mass analyzed by an orthogonal time-of-flight mass spectrometer (Accu-TOF, JEOL, Musashino, Tokyo, Japan) over the *m/z* range of 100–10,000. The voltage difference between the orifice and the skimmer was kept at 40 V in order to suppress the collision-induced dissociation of ions sampled into the first vacuum chamber.

The laser spray is monitored by a CCD camera (Toshiba, type IK-52V, Tokyo, Japan), and the image is displayed on a CCD monitor with 200× magnification. High-quality imaging of the capillary tip and spray was found to be extremely useful for the optimization of experimental conditions, such as the N_2-nebulizer gas flow rate, the laser power, the high voltage applied to the capillary, etc.

A bubble is frequently seen in the liquid cone in electrospray. This is almost certainly due to oxidation of H_2O to O_2 taking place near the tip of the stainless steel capillary [18].

$$2H_2O \rightarrow 4H^+ + O_2 + 4e \quad (1)$$

The bubble typically appears every 20 ~ 30 s. The bubble nucleation, its growth, and blow-off cause periodic fluctuation of the Taylor cone and some instability of the ion signal.

All chemicals were of analytical grade and obtained commercially. The water solvent was prepared by purification of the distilled water with ion exchange resins (Millipore, Simpli Lab., Billerica, MA). The Swiss-Prot sequence identifier for the hen egg lysozyme is LYC_CHICK and its primary accession number is P00698. The Swiss-Prot sequence identifier for the horse heart myoglobin is MYG_HORSE and its primary accession number is P68082.

Results and Discussion

In the present work, the laser beam was focused to cover the entire the 0.3 mm diameter front face of the stainless steel electrospray capillary, as described in the Experimental section. Relative to the previous laser spray setup, the laser power density was decreased by more than a factor of twenty. As a result of this change, ion signals are much more stable and mass spectra more reproducible. The appearance of the electrospray meniscus is also quite different. At the higher power density in the previous setup, violent ejections of jets and droplets were accompanied by an audible crackling noise. In the present setup, a smoother and quiescent evaporation of aqueous solution on the meniscus is observed on the video monitor, and there is no audible noise. It is also much easier to adjust the laser beam to the center of the stainless steel capillary without damaging the tip of the capillary by overheating.

Figure 1 shows the dependence of protein signal intensity on laser power for a 10^{-6} M hen egg white lysozyme solution in water. With laser power of 0 W (i.e., normal electrospray), no lysozyme signal is detected. The signal appears at 0.6 W (850 W/cm^2), shows a rapid increase and reaches a maximum with laser power value of ~2 W (~3×10^3 W/cm^2). Due to fast vaporization by laser heating, the liquid is barely protruding from of the stainless steel capillary tip at a power of 2 W. The sudden loss of signal above 2 W coincides with the disappearance of any visible liquid on the tip of the capillary.

That the ion signal should disappear when the liquid surface retreats into the capillary is reasonable because the inside of the metal capillary is nearly field-free, and separation of positive and negative ions will not occur. Thus, any droplet formation would likely have to be electrospray-driven, and this would require a strong electric field as well.

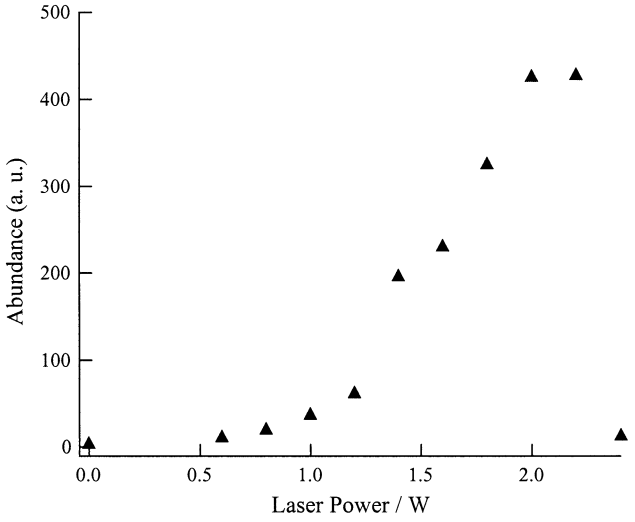

Figure 1. Dependence of protein ion signal intensity on laser power for an aqueous solution of 10^{-6} M hen egg white lysozyme. The flow rate of N_2 nebulizer gas is adjusted to obtain maximum ion signal. The sample flow rate is 10 μL/min. Voltage applied to the capillary is 2.8 kV. The voltage drop between the sampling orifice and the skimmer is 40 V.

Figure 2 depicts the lysozyme signal intensity as a function of protein concentration in electrospray (0 W, i.e., laser off) and laser spray (2 W). Compared to electrospray, it is seen that laser spray produces more than one order of magnitude increase in ion signal for concentrations $\leq 10^{-5}$ M. As a result, the detection limit is about 20 times lower in laser spray, i.e., 3×10^{-7} M versus 5×10^{-6} M in electrospray. However, the advantage of laser spray over electrospray becomes less prominent with increasing sample concentration and the signal intensities are comparable above 10^{-4} M.

The rapid evaporation caused by the laser irradiation causes enrichment of analyte near to the surface, and this is likely a major reason for the rapid increase in ion signal with laser power observed in Figure 1. The strongest ion signal was obtained at the laser power when the liquid droplet at the tip of the capillary was small, but still present, and this situation should give maximum enrichment. Assuming that analyte enrichment is the only factor responsible for the intensity difference between electrospray and laser spray, enrichment factors can be estimated from the data in Figures 1 and 2. For example, the signal obtained from a 1×10^{-6} M lysozyme solution with laser spray at 1.6 W is about 230, Figure 1. In electrospray, a protein concentration of 6×10^{-6} M is required to obtain the same signal level. Thus, the calculated enrichment factor is 6. It is found that calculated enrichment factor increases approximately linearly from 1.7 at 0.6 W to 7.5 at 2.0 W. Extrapolation to unity enrichment occurs at 0.4 W, and this indicates that the first 0.4 W of laser power is ineffective in promoting analyte enrichment.

It is noteworthy that the signal in laser spray continues to increase with lysozyme concentration until about 5×10^{-5} M. This corresponds to 4×10^{-4} M, after enrichment, which is well above the protein concentration, 1×10^{-4} M, at which the electrospray signal saturates. Above 5×10^{-5} M lysozyme concentration, there is a drastic decrease in the laser spray signal. This behavior is characteristic of laser spray [19]. In contrast, only a leveling off is observed in electrospray, typically above 10^{-5} M. Thus, the source for the signal decrease in laser spray should be sought in a process that doesn't occur in electrospray. It is possible that the laser-driven enrichment to high analyte and electrolyte concentrations near the liquid surface is responsible for this effect.

Figure 3 shows the electrospray (laser off) and laser spray (laser power: 2.0 W) mass spectra for 10^{-5} M aqueous solution of hen egg white lysozyme, with and without the addition of 10^{-2} M CH_3COONH_4. The upper trace in Figure 3a displays the electrospray spectrum (no laser) obtained without added CH_3COONH_4. The maximum charge state for lysozyme is +10. In the limit hypothesis that every negative charge (when working in the positive-ion mode) is protected against neutralization by intramolecular interactions in the folded protein, the observed number of charges in electrospray would simply correspond to the difference between the numbers of basic and acidic residues in the primary structure (except for buried, neutral His residues) [20]. Among the 129 amino acid residues in hen egg white lysozyme, 18 are basic (11 Arg, 6 Lys, 1 His), and 9 are acidic (7 Asp, 2 Glu). Considering also the charges on the terminal amino and carboxyl groups and that the histidine is buried (www.rcsb.org /pdb/; ID: 193L), the net positive charges for the native lysozyme would be +(18-1) − 9 = +8. This value is indeed close to the observed maximum charge

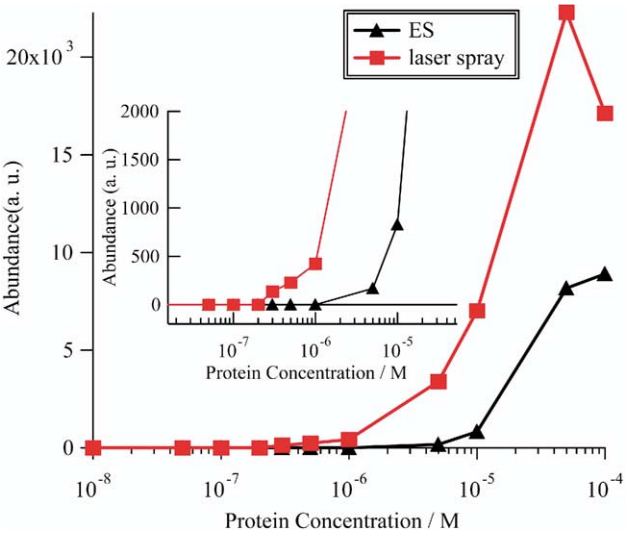

Figure 2. Signal intensity as a function of the concentration of lysozyme in aqueous solution in electrospray and laser spray. The flow rate of N_2 nebulizer gas is adjusted to obtain maximum ion signal. Laser spray results are for 2.0 W laser power. The sample flow rate is 10 μL/min. The voltage drop between the sampling orifice and the skimmer is 40 V.

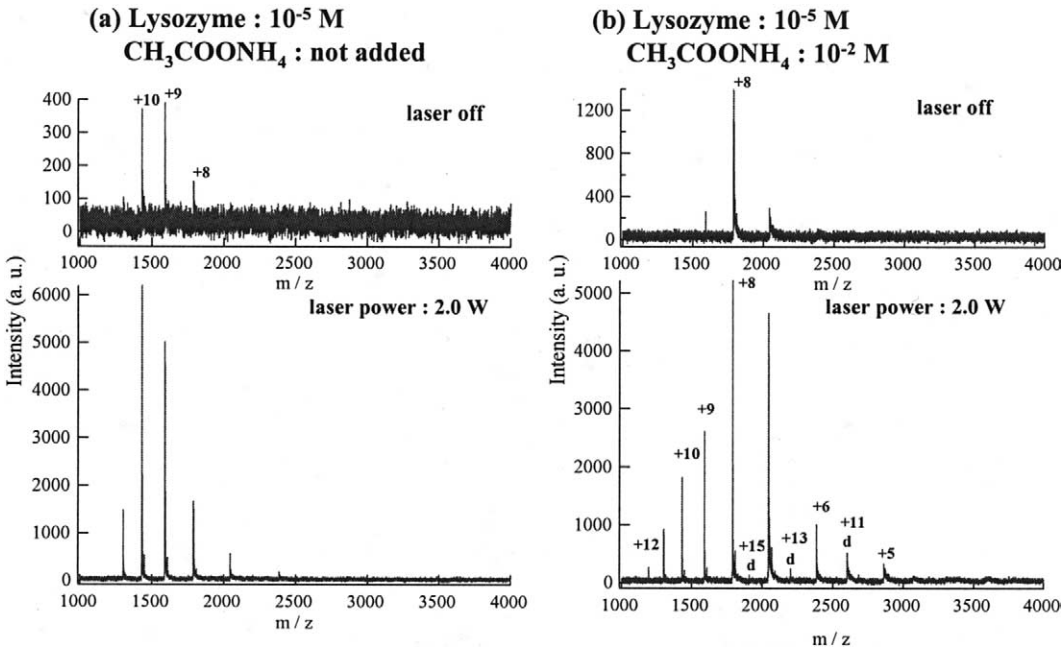

Figure 3. Electrospray (laser off) and laser spray (laser power of 2.0 W) mass spectra for aqueous solution of 10^{-5} M hen egg white lysozyme. (**a**) no CH_3COONH_4 is added, (**b**) 10^{-2} M CH_3COONH_4 is added in the aqueous solution. The sample flow rate is 10 μL/min. The flow rate of the nebulizer gas N_2 are 0.5 L/min for laser off and 1.0 L/min for laser on. Voltage applied to the capillary is 2.8 kV. The voltage drop between the sampling orifice and the skimmer is 40 V. The symbol "d" denotes lysozyme dimer.

state. This agreement may be reasonable, considering that lysozyme is a very tightly folded globular protein.

Work by de la Mora [21] provides strong evidence that charged globular protein ions in electrospray are formed according to the charged residue model. Maximum charge states, Z_{obs}, reported in the literature for globular intact proteins with mass from 10^4 Da to above 10^6 Da and sprayed from water as the major solvent, were compiled. It was found that the Z_{obs} values were close or equal to the maximum charge, Z_{RS}, that an aqueous droplet of same radius as that of the protein can carry. The value of Z_{RS} for a water droplet of radius R is calculated using eq 2,

$$Z_{RS} = (8\pi/e)(\gamma\varepsilon_0 R^3)^{1/2} \quad (2)$$

where γ is the surface tension of water (0.072 N/m), ε_0 the electrical permittivity of vacuum (8.8×10^{-12} C^2/J m), and e the elementary charge (1.6×10^{-19} C). R is the radius calculated for the protein, assuming that the protein is spherical and has a density of 1 g/cm^3. For lysozyme, it is found that Z_{RS} is between 9 and 10. Kebarle and coworkers added different ammonium acetate salts to protein solutions [22]. With increasing gas-phase basicity GB of the conjugate base, they found that there was a progressive decrease in the observed charge states. This provides additional strong evidence that the **maximum number of charges** can be rationalized by the charged residue model.

The lower trace in Figure 3a shows the laser spray mass spectrum of lysozyme, with no added ammonium acetate, at a laser power of 2.0 W. It is seen that the lysozyme charge distribution remains essentially unchanged (a careful inspection shows that the distribution is marginally wider). This strongly supports the indication that the protein retains its native structure, i.e., a laser power of 2 W is not enough to induce the denaturation of lysozyme. This is reasonable because, as already stated, lysozyme has a tightly folded structure with four disulfide linkages.

Figure 3b demonstrates the effect on lysozyme mass spectra of adding 10^{-2} M CH_3COONH_4 to the protein solution. The upper trace shows that in electrospray (i.e., no laser), the charge distribution shifts to lower charge states compared with the spectra obtained without the addition of CH_3COONH_4, see Figure 3a, upper trace. This charge reduction may be attributable to salt formation of $(\text{lysozyme} + \text{nH})^{n+}$ with the acetate ion CH_3COO^- leading to a reduction of number of positive charges.

$$\begin{aligned}(\text{lysozyme} + \text{nH})^{n+} + CH_3COO^- &\rightarrow \\ (\text{lysozyme} + \text{nH})^{n+} \cdots CH_3COO^- &\rightarrow \\ (\text{lysozyme} + (\text{n}-1)\text{H})^{(n-1)+} + CH_3COOH \quad (3)\end{aligned}$$

Mirza et al. investigated the effects of anions on the positive ion electrospray mass spectra of peptides and proteins [23]. They found that certain anionic species in the spray solutions caused a marked decrease in the net

average charge of peptide and protein ions in the mass spectra compared with the average charge measured in the absence of these anions, with the propensity for neutralization following the order: $CCl_3COO^- > CF_3COO^- > CH_3COO^- \approx Cl^-$. It should be noted that the observed order is that of the negative-charge delocalization in the anionic species. The size of the hydration shell for the hydrated negative ions in aqueous solution becomes smaller with the negative-charge dispersal in the negative ion moiety. The stronger neutralization ability of less-hydrated negative ions may be due to the fact that the less-hydrated ions can approach closer to the positive-ion site because they have thinner hydration shells. The thinner the hydration shell, the smaller the energy barrier for the proton transfer reaction in solution.

The lower trace in Figure 3b shows that the charge distribution with laser spray (laser power: 2 W) becomes much wider than that obtained with electrospray, upper trace. This broadening is observed with 10^{-2} M CH_3COONH_4 and is in sharp contrast to the results obtained in the absence of CH_3COONH_4. It is apparent that the laser-induced heating causes denaturation of lysozyme in aqueous solution, but only in the presence of 10^{-2} M CH_3COONH_4. An increase in the propensity for heat-induced protein denaturation with the addition of salt seems counterintuitive, because higher order structures are generally stabilized in solution by the addition of moderate concentrations of salt [24]. Mirza and Chait studied the thermal denaturation of proteins in electrospray ionization using a heated capillary electrospray ionization source [24]. They found that the addition of 5 mM CH_3COONH_4 to a solution of water/methanol (1:1, vol/vol) promoted thermal denaturation of lysozyme. They concluded that the addition of ammonium acetate has the effect of increasing the lifetime of electrosprayed droplets attributable to a decrease in the rate of solvent evaporation, thus increasing the time available for heat transfer and denaturation. The mechanism of energy transfer to the liquid and sprayed liquid droplets is of paramount importance for laser spray and a further investigation of this aspect is now in progress in our laboratory.

The main effect of laser irradiation on dissolved protein is heating. The time that the proteins spend at an increased temperature should be of the order of milliseconds. Therefore, it is of interest to consider the rates of thermal denaturation rates of lysozyme. The denaturation of a protein is affected by pH, as well as temperature. With lowering of pH, the temperature for denaturation decreases. Benesch et al. investigated the thermal denaturation of lysozyme using nanoelectrospray mass spectrometry [25]. They found that the melting point of lysozyme in aqueous solution at pH 2.0 is 43.0 ± 0.6 °C. Creighton measured the unfolding rate constant of lysozyme at pH = 3.0 as a function of temperature [26]. Extrapolation of the data indicates that rate constants of 10^3 s^{-1} may be achieved at temperatures above approximately 110 °C. This is roughly consistent with the present results.

It should be noted that the lysozyme dimer ions $(2\ M + nH)^{n+}$ with n = 10–15 are observed in Figure 3b with a laser power of 2.0 W. In contrast, no dimers are detected in the absence of ammonium acetate or in electrospray mode. The appearance of dimers is likely attributable to both the heat-induced denaturation and the enrichment of lysozyme by laser-induced evaporation. Generally, proteins are nondiscriminatory in that they interact and bind with a variety of species such as other proteins, peptides, oligo-nucleotides, metal ions, and other small molecules [27]. Because lysozyme denatures at a laser power of ~2.0 W, its abundant hydrophobic regions may be exposed in solution and this may increase the tendency to form dimers. In our recent work [28] it was found that irradiation of 10.6 μm laser is not effective to dissociate hydrophobic bonds in clusters of chemically modified cyclodextrin molecules dissolved in aqueous solution. This seems reasonable because absorption of 10.6 μm infrared light is mainly due to intermolecular hydrogen bonds in water. Hydrophobic interaction of proteins is weaker in the gas phase than in aqueous solution, because this type of interaction is strongly favored by an increase in the entropy of the aqueous solvent. Thus the effects of laser irradiation on the dissociation of noncovalent bonds, including hydrophilic and hydrophobic interactions, must be evaluated from various points of view. The study on the laser spray for noncovalent complexes such as protein–protein, drug–protein, drug–DNA, etc. is now in progress in our laboratory [29].

In the range of laser power from 0 to 1.6 W, and in the presence of 10^{-2} M CH_3COONH_4, no unfolding of lysozyme is observed (results not shown). Since the unfolding of proteins is seen only above a critical laser power, it should be possible to investigate the stabilities of noncovalently bonded biological macromolecules by tuning the laser power. Because of the demonstrated ability of laser spray to control, in real time, the denaturation of proteins such as lysozyme, it is of considerable interest to apply laser spray to the characterization of noncovalent complexes. Here, myoglobin, which is a noncovalent complex of heme and globin, was investigated as a function of laser power.

Figure 4 shows photographs of the spray of a 10^{-5} M horse heart myoglobin aqueous solution with laser off (electrospray) and on with laser powers of 1.6, 1.8, and 2.0 W, together with the corresponding mass spectra. For electrospray (laser off), only peaks attributable to holo-myoglobin (denoted as "h" in Figure 4) with +8 and +7 charge states are observed.

Among the 153 amino acid residues in horse heart myoglobin, 32 are basic (2 Arg, 19 Lys, 11 His), and 21 are acidic (8 Asp, 13 Glu). X-ray crystallographic data [30–34] and information in RCSB protein databank (www. rcsb.org/pdb/) show that in native myoglobin all acidic and basic residues are solvent-accessible, with the exception of three His residues. If all solvent-

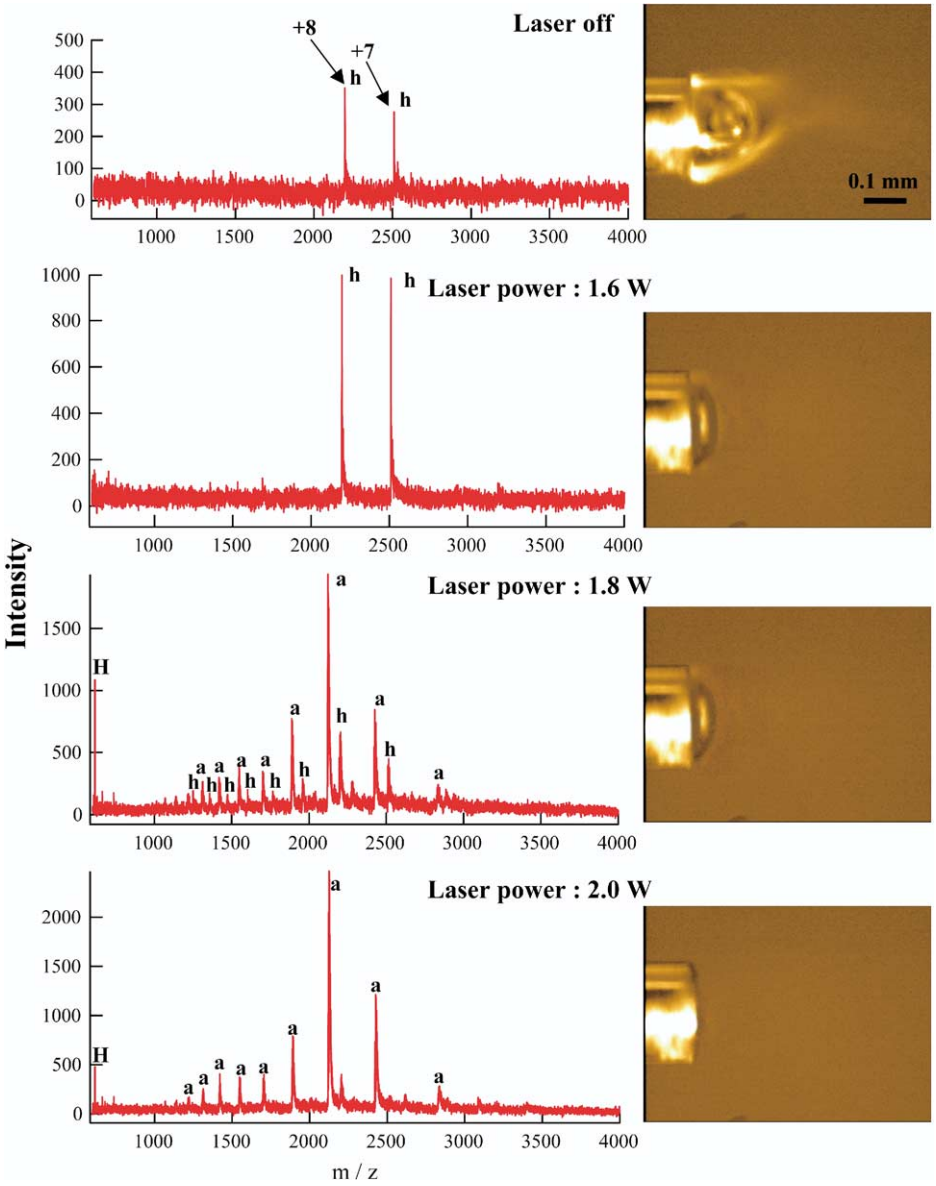

Figure 4. Photographs of 10^{-5} M horse heart myoglobin aqueous solution flowing out of the tip of the stainless steel capillary with laser off (electrospray) and on, with laser power values of 1.6, 1.8, and 2.0 W together with the mass spectra obtained at the corresponding laser powers. The sample flow rate is 10 μL/min. The flow rates of the nebulizer gas N_2 are 0.5 L/min for laser off and 1.0 L/min for laser on. The voltage applied to the capillary is 2.8 kV. The voltage drop between the sampling orifice and the skimmer is 40 V. The symbols "H", "h", and "a" in the figures denote heme^{+1} (*m/z* 616), holo-myoglobin, and apo-myoglobin, respectively.

accessible residues were to be ionized, the net charge of native myoglobin would be +8, i.e., the number of chargeable basic residues (+32-3 = +29), minus the number of acidic residues (21), plus the terminal amino group, minus the terminal carboxyl group, i.e., +29-21 + 1-1 = +8. As in the case of lysozyme, this value perfectly matches the maximum charge state of +8 for electrosprayed and laser sprayed native myoglobin in Figure 4 (top panels). Inspection of myoglobin x-ray structural models also reveals that in the native conformation, many positively and negatively charged residues are paired with a distance between charge sites equal to or less than 5 Å [30, 32, 35, 36]. These pairs are interacting via salt bridges, which contribute to the stability of the tertiary structure of the native protein.

It is seen in Figure 4, this with increase of the laser power to 1.6 W, the Taylor cone becomes smaller and round-shaped. Liquid spallation was not observed on the surface, as discussed above. The formation of finer liquid droplets for laser spray than for electrospray were seen around the center of the convex liquid surface as a decrease in the scattering of visible light. Such a decrease in droplet size in laser spray is associated with enhanced ion signals. Unfortunately, the

resolution of photograph taken by the CCD camera is not sufficient to determine the change in size of the sprayed droplets (Figure 4, first and second panels). At a laser power of 1.6 W, the myoglobin charge distribution is narrow and essentially the same as for electrospray. This level of laser irradiation is not sufficient to induce denaturation of the protein.

Laser spray mass spectra of myoglobin changed drastically when the laser power was increased from 1.6 W to 1.8 W, as shown in the third panel in Figure 4. With only a 0.2 W increment of laser power, the intensities of holo-myoglobin ions with +7 and +8 charges decreased and peaks of apo-myoglobin (denoted with "a" in Figure 4) with higher charge states up to +13 as well as heme^{+1} (*m/z* 616) appeared. Clearly, extensive denaturation of myoglobin occurs with concomitant loss of the heme group. As with denaturation of lysozyme, there is a sudden onset of denaturation at a specific laser power value. This suggests that the thermal denaturation of holo-myoglobin is a highly cooperative process with a rather high energy barrier. In addition to the appearance of apo-myoglobin ions and heme^{+1}, higher charge states of holo-myoglobin up to +14 are newly observed. This indicates the presence of myoglobin that is substantially unfolded but still retains its heme group. This means that laser spray is capable of detecting **transient intermediates** during the denaturation of holo-myoglobin. This is made possible by the millisecond-range excitation and detection processes.

The presence of unfolded holo-myoglobin suggests that the thermally induced denaturation of the heme-protein complex starts with unfolding of the protein, but with the heme pocket still preserved. This scenario is in agreement with the experimental observation that the transient holo-myoglobin unfolding intermediate has a largely intact heme binding pocket, whereas other regions of the protein have lost their native structure [37, 38].

When the laser power is further increased to 2.0 W (bottom panel in Figure 4), the liquid on the tip of the capillary almost disappears and the liquid droplets sprayed are barely seen by the video microscope, i.e., the finest liquid droplets are formed at the highest laser power. In the 2.0 W mass spectrum, multiply charged apo-myoglobin ions with +6 to +14 charges are observed as major ions, while the unfolded holo-myoglobin peaks have almost disappeared.

Surprisingly, the charge distribution for apo-myoglobin has two distinct components. A wide distribution extends to high charge states, and a narrow distribution consists of high intensity peaks for +7 to +8. The wide distribution is indeed expected, as fully unfolded apomyoglobin should be formed according to the reported mechanism [37] in which the protein partially unfolds before the heme is lost. The protein may maintain the heme pocket even though the heme has detached. Sage et al. performed spectroscopic studies of myoglobin at low *pH* [39]. These authors suggested that the distal heme pocket retains significant structural integrity following the native structure to unfolded conformational change. The retention of an element of tertiary structure (the heme pocket) in the face of a substantial loss of secondary structure (α-helical content) suggests that the primary disorganization of the secondary structure takes place in a region remote from the heme site.

The narrow apo-myoglobin charge distribution at low charge states is more difficult to explain. It does suggest the existence of compact folded apo-myoglobin, which could be formed either by the refolding of previously unfolded apo-myoglobin or by direct dissociation of native myoglobin to heme and tightly folded apo-myoglobin.

The results above demonstrate that laser spray is able to dissociate noncovalent complexes. At the same time, no fragmentation of covalent bonds has been observed. The ability to selectively dissociate noncovalent bonds is unique to electrospray. This is because laser spray relies on the absorption of 10.6 μm infrared laser, mainly by water solvent. With water solvent temperature rising [40], the absorption coefficient decreases drastically, and thus the heating of biological samples is self-limiting. This makes it possible to extract labile biological molecules in solution to the gas phase under very mild conditions.

Using laser spray, it is possible to monitor the denaturation of proteins and the dissociation of noncovalent bond complexes in seconds by switching the laser on and off. The laser spray is highly suitable for the observation of transient intermediates of proteins and noncovalent complexes by the fine control of the laser power. The selective dissociation of noncovalent bonds by laser spray will open the venue for the unequivocal differentiation of noncovalent and covalent macromolecular complexes. Owing to the ability to finely adjust the laser power, laser spray promises to become a versatile method for quick screening of biologically important noncovalent complexes, such as enzyme–substrate, receptor–ligand, host–guest, protein–nucleic acid [17], etc. The field of biochemistry would greatly benefit from a method that in a rapid and sensitive manner can provide information on macromolecular interactions.

Conclusions

The use of a relatively low CO_2-laser irradiance level in laser spray demonstrated significant advantages compared with both electrospray and the previously investigated high-irradiance laser spray method. With a laser power of $\leq$2 W and a focal spot size of $\sim$0.3 mm, which covered the entire front surface of the electrospray capillary, the irradiance is $\sim 3 \times 10^3$ W/cm^2. Unlike the previous high-irradiance ($\sim 6 \times 10^4$ W/cm^2) laser spray experiments in which extensive vapor explosions take place in the liquid surface, the low irradiance resulted in a quiescent and smooth vaporization of aqueous solutions. The "evaporation mode" laser spray method

produced, thus far, the best data obtained in our laboratory with laser-irradiated electrospray, yielding higher and more stable signal intensities. In our present investigation, mass spectra of lysozyme and myoglobin have been obtained using an orthogonal TOF mass spectrometer. Signal intensities increase with laser irradiance. At low protein concentrations, this increase is more than one order of magnitude. At high laser power, denaturation of both lysozyme and myoglobin and, in the case of myoglobin, dissociation into apo-myoglobin and heme, were accomplished.

The merits of evaporation-mode laser spray may be summarized as follows:

1. The method is most suitable for aqueous solution because water has a high absorption coefficient ($\sim 10^3$ cm^{-1}) [16] for 10.6 μm infrared light.
2. Laser irradiation makes it easier to spray aqueous solutions because of the decrease of viscosity and surface tension of the liquid at increased temperature.
3. The evaporative mode laser spray is characterized by high and stable ion signals.
4. Enrichment of the analyte takes place on the surface of the liquid effusing out of the capillary because of selective vaporization of water solvent in aqueous solution, and this results in increased ion signals.
5. Denaturation of proteins can be induced above a well-defined laser power threshold.

Considering the above merits, the evaporation-mode laser spray method appears to be ideally suited to probe the stabilities of biomolecules and noncovalent complexes in aqueous solutions.

Acknowledgments

This work was supported by a Grant-in-Aid from the Japanese Ministry of Education, Science, and Culture (Special Coordination Funds for the Promotion of Science and Technology, no. 20403010). The authors are indebted to Professor Satoko Akashi of the Yokohama City University for her illuminating discussions.

References

1. Skripov, V. P. *Metastable Liquids*; Wiley, New York, NY, 1974; p 177.
2. Shepherd, J. E.; Sturtevant, B. *Fluid Mech.* **1982**, *121*, 379–402.
3. Kafalas, P.; Ferdinand, A. P., Jr. *Appl. Opt.* **1973**, *12*, 29–33.
4. Hiraoka, K.; Murata, K.; Aizawa, K.; Matsushita, F.; Fukasawa, H.; Sato, T. *Rapid Commun. Mass Spectrom.* **1997**, *11*, 474–478.
5. Wattenberg, A.; Sobbot, F.; Brutschy, B. *Rapid Commun. Mass Spectrom.* **2000**, *14*, 859–861.
6. Wattenberg, A.; Sobott, F.; Barth, H.-D.; Brutschy, B. *Int. J. Mass Spectrom.* **2000**, *203*, 49–57.
7. Hiraoka, K.; Katayama, S.; Aizawa, K.; Matsushita, F.; Fukasawa, H. *J. Mass Spectrom. Soc. Jpn.* **1995**, *43*, 265–277.
8. Hiraoka, K. *Rapid Commun. Mass Spectrom.* **1992**, *6*, 463–468.
9. Hiraoka, K.; Fukasawa, H.; Matsushita, F.; Aizawa, K. *Rapid Commun. Mass Spectrom.* **1995**, *9*, 1349–1355.
10. Hiraoka, K. *J. Mass Specrtom.* **2004**, *39*, 341–350.
11. Hiraoka, K.; Asakawa, Y.; Ueda, K.; Hori, A.; Sakai, T.; Okazaki, S.; Nakamura, M. *Rapid Commun. Mass Spectrom.* **2002**, *16*, 1100–1105.
12. Hiraoka, K.; Saito, S.; Katsuragawa, J.; Kudaka, I. *Rapid Commun. Mass Spectrom.* **1998**, *12*, 1170–1174.
13. Hiraoka, K.; Asakawa, Y.; Yamamoto, Y.; Nakamura, M.; Ueda, K. *Rapid Commun. Mass Spectrom.* **2001**, *15*, 2020–2026.
14. Kudaka, I.; Kojima, T.; Saito, S.; Hiraoka, K. *Rapid Commun. Mass Spectrom.* **2000**, *14*, 1558–1562.
15. Kojima, T.; Kudaka, I.; Sato, T.; Asakawa, T.; Akiyama, R.; Kawashima, Y.; Hiraoka, K. *Rapid Commun. Mass Spectrom.* **1999**, *13*, 2090–2097.
16. Vogel, A.; Venugopalan, V. *Chem. Phys.* **2003**, *103*, 577–644.
17. Takamizawa, A.; Itoh, Y.; Osawa, R.; Iwasaki, N; Nishimura, Y.; Akashi, S.; Hiraoka, K. *J. Mass Spectrom.* **2004**, *39*, 1053–1058.
18. van Berkel, G. J.; Asano, K. G.; Schnier, P. D. *J. Am. Soc. Mass Spectrom.* **2001**, *12*, 853–862.
19. Hiraoka, K.; Asakawa, Y.; Kawashima, Y.; Okazaki, S.; Nakamura, M.; Yamamoto, Y.; Takamizawa, A. *Rapid Commun. Mass Spectrom.* **2004**, *18*, 2437–2442.
20. Grandori, R. *J. Mass Spectrom.* **2003**, **38**, 11–15.
21. de la Mora, J. F. *Anal. Chim. Acta* **2000**, *406*, 93–104.
22. Verkerk, U. H.; Peschke, M.; Kebarle, P. *J. Mass Spectrom.* **2003**, *38*, 618–631.
23. Mirza, U. A.; Cohen, S. L.; Chait, B. T. *Anal. Chem.* **1993**, *65*, 1–6.
24. Mirza, U. A.; Chait, B. T. *Int. J. Mass Spectrom. Ion Processes* **1997**, *162*, 173–181.
25. Benesch, J. L. P.; Sobott, F.; Robinson, C. V. *Anal. Chem.* **2003**, *75*, 2208–2214.
26. Creighton, T. E. *Biochem.* **1990**, *270*, 1–16.
27. Loo, J. A. *Mass Spectrom. Rev.* **1997**, *16*, 1–23.
28. Kuwabara, T.; Takamizawa, J.; Hiraoka, K., unpublished.
29. Shi, K; Takamizawa, A.; Akashi, S.; Hiraoka, K., unpublished.
30. Lehninger, A. L. Principles of Biochemistry; Worth Publishers: New York, NY, 1982; pp 150–151.
31. Kendrew, J. C.; Dickerson, R. E.; Strandberg, B. E.; Hart, R. G.; Davies, D. R.; Phillips, D. C.; Shore, V. C. *Nature* **1960**, *185*, 422–427.
32. Stryer, L.; *Biochemistry*; W. H. Freeman: New York, NY, 1988; pp 29–30, 143–174.
33. Takano, T. *J. Mol. Biol. Chem.* **1977**, *110*, 537–568.
34. Rothgeb, T. M.; Gurd, F. R. N. In *Methods in Enzymology*; Vol. LII. *Biomembranes* Part C; Fleisher, S; Packer, L., Eds.; Academic: New York, NY, 1978; pp 473–486.
35. Ghélis, C.; Yon, J. Protein Folding; Academic Press: New York, NY, 1982.
36. Feng, R; Konishi Y. *J. Am. Soc. Mass Spectrom.* **1993**, *4*, 638–645.
37. Konermann, L.; Rosell, F. I.; Mauk, A. G.; Douglas, D. J. *Biochemistry* **1997**, *36*, 6448–6454.
38. Sogbein, O. O.; Simmons, D. A.; Konermann, L. *J. Am. Soc. Mass Spectrom.* **2000**, *11*, 312–319.
39. Sage, J. T.; Morikis, D.; Champion, P. M. *Biochemistry* **1991**, *30*, 1227–1237.
40. Cormier, J. G.; Ciurylo, R.; Drummond, J. R. *J. Chem. Phys.* **2002**, *116*, 1030–1034.